

Prompting Lipschitz-constrained network for multiple-in-one sparse-view CT reconstruction

Baoshun Shi, *Senior Member, IEEE*, Ke Jiang, Qiusheng Lian, Xinran Yu, and Huazhu Fu, *Senior Member, IEEE*

This document is organized as follows. We first report the experimental results in Sec. I, and then provide the detailed proofs in Sec. II.

I. EXPERIMENTAL RESULTS

To further evaluate the effectiveness of our SVCT reconstruction algorithm, we supplement the comparison results of different algorithms for the SVCT reconstruction task, as shown in Figs. 1-5.

The reconstruction results of various SVCT reconstruction methods with 180 projection views on the AAPM dataset are presented in Fig. 1. It can be observed that the RED-CNN and CNNMAR demonstrate promising performance in removing streak artifacts, but they still suffer from some loss of fine image textures. In contrast, our proposed method consistently preserves fine details. Furthermore, we present some reconstructions achieved by these algorithms and the corresponding magnitude images of the reconstruction error in Figs. 2-5. Specifically, Fig. 2 and Fig. 3 display that the reconstructed CT images achieved by the proposed PromptCT obtain more tissue details and preserve the enriched structure information in terms of visual quality, while other algorithms suffer from severe blurring or secondary artifacts. Furthermore, the magnitude images of the reconstruction error indicate that PromptCT exhibits a closer resemblance to the original image than MLipCT, suggesting the effectiveness of explicit prompts in the multiple-in-one SVCT reconstruction task. From the magnified details in Fig. 4 and Fig. 5, it is evident that both LipCT and PromptCT exhibit enhanced reconstruction accuracy compared to other algorithms. The magnitude image of the reconstruction error for PromptCT shows pixel errors of much smaller magnitude than those of other algorithms.

This work was supported by the National Natural Science Foundation of China under Grants 62371414 and 62571473, by the Hebei Natural Science Foundation under Grant F2025203070, and by the Hebei Key Laboratory Project under Grants 202250701010046. The authors thank the anonymous reviewers for constructive suggestions. (*Baoshun Shi and Ke Jiang contributed equally to this work.*) (*Corresponding authors: Baoshun Shi and Qiusheng Lian.*)

Baoshun Shi, Ke Jiang, and Qiusheng Lian are with the School of Information Science and Engineering, Yanshan University, Qinhuang Dao, 066004, Hebei province, China (e-mail: shibaoshun@ysu.edu.cn, liangs@ysu.edu.cn).

Xinran Yu is with the Beijing Advanced Innovation Center for Imaging Technology, Capital Normal University, Beijing 100048, China.

Huazhu Fu is with the Institute of High Performance Computing (IHPC), Agency for Science, Technology and Research (A*STAR), Singapore 138632.

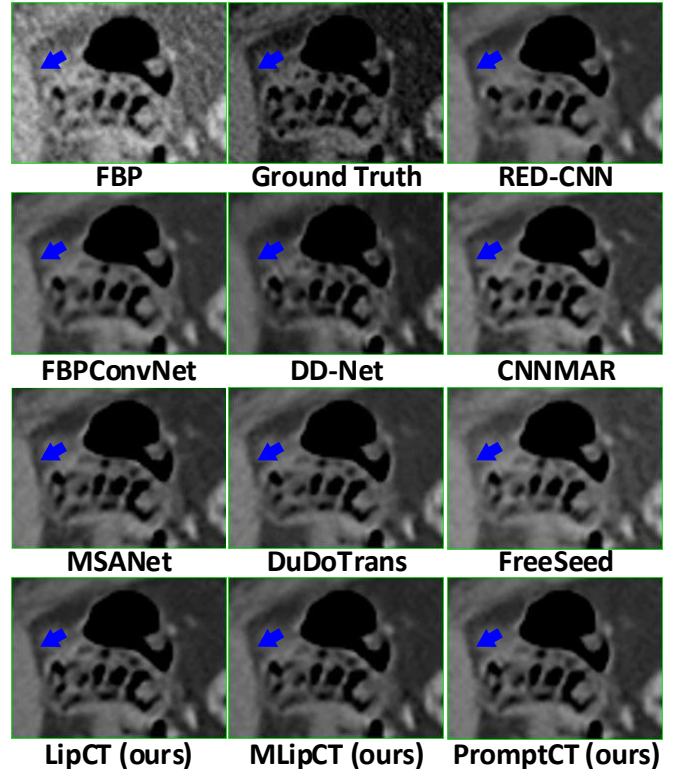


Fig. 1. Visual comparison of SVCT reconstruction methods with 180 projection views on AAPM dataset. The display window is [-175, 500] HU. Regions of interest are zoomed in for better viewing.

II. THE PROOFS

A. The proof of Lemma 1

Define $\mathbf{W} \in \mathbb{R}^{M \times N}$ as the analysis frame and $\mathbf{W}^T \in \mathbb{R}^{N \times M}$ as the synthesis frame, we can construct the following inequality:

$$\begin{aligned} & \|\mathbf{W}^T \mathbf{W} \mathbf{x} - \mathbf{W}^T T_{\varepsilon(\sigma)}(\mathbf{W} \mathbf{x})\|_2^2 \\ & \leq \|\mathbf{W}^T\|_2^2 \|\mathbf{W} \mathbf{x} - T_{\varepsilon(\sigma)}(\mathbf{W} \mathbf{x})\|_2^2 \end{aligned} \quad (1)$$

where $\|\mathbf{W}^T\|_2^2 = \lambda_{max}(\mathbf{W} \mathbf{W}^T)$ and $\lambda_{max}(\cdot)$ represents the maximum eigenvalue of $\mathbf{W} \mathbf{W}^T$. We assume that the maximum eigenvalue of $\mathbf{W} \mathbf{W}^T$ is τ_0 , the upper bound of Eqn. (1) can be further determined by

$$\|\mathbf{W}^T \mathbf{W} \mathbf{x} - \mathbf{W}^T T_{\varepsilon(\sigma)}(\mathbf{W} \mathbf{x})\|_2^2 \leq \tau_0 \|\mathbf{W} \mathbf{x} - T_{\varepsilon(\sigma)}(\mathbf{W} \mathbf{x})\|_2^2. \quad (2)$$

Equation (2) can be recast as

$$\|\mathbf{W}^T \mathbf{W} \mathbf{x} - \mathbf{W}^T T_{\varepsilon(\sigma)}(\mathbf{W} \mathbf{x})\|_2^2 \leq \tau_0 \|\mathbf{W} \mathbf{x} - T(\mathbf{W} \mathbf{x}, \mathbf{e})\|_2^2. \quad (3)$$

Here, we use \mathbf{e} to represent the threshold vector whose elements are utilized for shrinking $\mathbf{W} \mathbf{x}$. Let $(\mathbf{W} \mathbf{x})_i$ represents the i -th element of $\mathbf{W} \mathbf{x}$ and ε_i denotes the i -th element of \mathbf{e} . The soft thresholding operator $T[(\mathbf{W} \mathbf{x})_i, \varepsilon_i]$ is defined as

$$T[(\mathbf{W} \mathbf{x})_i, \varepsilon_i] = \begin{cases} (\mathbf{W} \mathbf{x})_i + \varepsilon_i, & (\mathbf{W} \mathbf{x})_i < -\varepsilon_i \\ 0, & |(\mathbf{W} \mathbf{x})_i| \leq \varepsilon_i \\ (\mathbf{W} \mathbf{x})_i - \varepsilon_i, & (\mathbf{W} \mathbf{x})_i > \varepsilon_i. \end{cases} \quad (4)$$

We consider the shrinking process $T(\mathbf{W} \mathbf{x}, \mathbf{e})$, one of the following situations will happen.

C1: Any element of $\mathbf{W} \mathbf{x}$ satisfies $(\mathbf{W} \mathbf{x})_i < -\varepsilon_i$, then $T(\mathbf{W} \mathbf{x}, \mathbf{e}) = \mathbf{W} \mathbf{x} + \mathbf{e}$. Therefore,

$$\|\mathbf{W} \mathbf{x} - T(\mathbf{W} \mathbf{x}, \mathbf{e})\|_2^2 = \|\mathbf{W} \mathbf{x} - \mathbf{W} \mathbf{x} - \mathbf{e}\|_2^2 = \|\mathbf{e}\|_2^2. \quad (5)$$

C2: Any element of $\mathbf{W} \mathbf{x}$ satisfies $|(\mathbf{W} \mathbf{x})_i| \leq \varepsilon_i$, then $T(\mathbf{W} \mathbf{x}, \mathbf{e}) = 0$. Therefore,

$$\|\mathbf{W} \mathbf{x} - T(\mathbf{W} \mathbf{x}, \mathbf{e})\|_2^2 = \|\mathbf{W} \mathbf{x} - 0\|_2^2 \leq \|\mathbf{e}\|_2^2. \quad (6)$$

C3: Any element of $\mathbf{W} \mathbf{x}$ satisfies $(\mathbf{W} \mathbf{x})_i > \varepsilon_i$, then $T(\mathbf{W} \mathbf{x}, \mathbf{e}) = \mathbf{W} \mathbf{x} - \mathbf{e}$. Therefore,

$$\|\mathbf{W} \mathbf{x} - T(\mathbf{W} \mathbf{x}, \mathbf{e})\|_2^2 = \|\mathbf{W} \mathbf{x} - \mathbf{W} \mathbf{x} + \mathbf{e}\|_2^2 = \|\mathbf{e}\|_2^2. \quad (7)$$

C4: Any two or all three of the above situations may occur. C4 is a union of C1, C2, and C3. Therefore, as long as we find the upper bound of $\|\mathbf{W} \mathbf{x} - T(\mathbf{W} \mathbf{x}, \mathbf{e})\|_2^2$ under the C1-C3, the upper bound of that under C4 will be determined. Hence, when C4 occurs, the upper bound of is the maximum upper bound of $\|\mathbf{W} \mathbf{x} - T(\mathbf{W} \mathbf{x}, \mathbf{e})\|_2^2$ the first three situations. Based on (5), (6), and (7), we have

$$\|\mathbf{W} \mathbf{x} - T(\mathbf{W} \mathbf{x}, \mathbf{e})\|_2^2 \leq \|\mathbf{e}\|_2^2. \quad (8)$$

Recall the definition of threshold vector $\mathbf{e} = \mathbf{c} \odot \mathbf{m}$, and each element of the proportional constant vectors \mathbf{c} has a limited range $c_i \in [c_{min}, c_{max}]$. Let $\varepsilon_{max} = c_{max} \cdot \sigma$ denote the maximum element of \mathbf{e} . Thus,

$$\|\mathbf{e}\|_2^2 \leq M \varepsilon_{max}^2 \leq M c_{max}^2 \sigma^2. \quad (9)$$

According to (3), (8), and (9), we can get

$$\|\mathbf{W}^T \mathbf{W} \mathbf{x} - \mathbf{W}^T T_{\varepsilon(\sigma)}(\mathbf{W} \mathbf{x})\|_2^2 \leq \tau_0 M \sigma^2 c_{max}^2 \leq M \sigma^2 L \quad (10)$$

where $L = \tau_0 c_{max}^2$. \blacksquare

B. The proof of Theorem 1

According to $\mathbf{x}_t = \alpha \mathbf{x}_0 + \alpha \beta \mathbf{W}^T T_{\varepsilon(\sigma)}(\mathbf{W} \mathbf{x}_{t-1})$, we have

$$\begin{aligned} \mathbf{x}_T &= \alpha \mathbf{x}_0 + \alpha \beta \mathbf{W}^T T_{\varepsilon(\sigma)}(\mathbf{W} \mathbf{x}_{T-1}), \\ \mathbf{x}_{T-1} &= \alpha \mathbf{x}_0 + \alpha \beta \mathbf{W}^T T_{\varepsilon(\sigma)}(\mathbf{W} \mathbf{x}_{T-2}), \\ &\dots \\ \mathbf{x}_1 &= \alpha \mathbf{x}_0 + \alpha \beta \mathbf{W}^T T_{\varepsilon(\sigma)}(\mathbf{W} \mathbf{x}_0). \end{aligned} \quad (11)$$

Furthermore, the ouput image $\mathcal{D}_\theta(\mathbf{x}_0; \sigma)$ is denoted as \mathbf{x}_T . The difference between the input image \mathbf{x}_0 and the ouput image \mathbf{x}_T satisfies

$$\begin{aligned} &\|\mathbf{x}_0 - \mathbf{x}_T\|_2^2 \\ &= \|\mathbf{x}_0 - \alpha \mathbf{x}_0 - \alpha \beta \mathbf{W}^T T_{\varepsilon(\sigma)}(\mathbf{W} \mathbf{x}_{T-1})\|_2^2 \\ &= \|\mathbf{x}_0 - \alpha \mathbf{x}_0 - \alpha \beta \mathbf{W}^T \mathbf{W} \mathbf{x}_{T-1} + \alpha \beta \mathbf{W}^T \mathbf{W} \mathbf{x}_{T-1} - \alpha \beta \mathbf{W}^T T_{\varepsilon(\sigma)}(\mathbf{W} \mathbf{x}_{T-1})\|_2^2 \\ &\leq \|\mathbf{x}_0 - \alpha \mathbf{x}_0 - \alpha \beta \mathbf{W}^T \mathbf{W} \mathbf{x}_{T-1}\|_2^2 \\ &\quad + \|\alpha \beta \mathbf{W}^T \mathbf{W} \mathbf{x}_{T-1} - \alpha \beta \mathbf{W}^T T_{\varepsilon(\sigma)}(\mathbf{W} \mathbf{x}_{T-1})\|_2^2. \end{aligned} \quad (12)$$

Based on $\alpha = \frac{1}{I + \beta \mathbf{W}^T \mathbf{W}}$ and **Lemma 1**, Eqn. (13) can be rewritten as

$$\begin{aligned} &\|\mathbf{x}_0 - \mathbf{x}_T\|_2^2 \\ &\leq \left\| \mathbf{x}_0 - \frac{1}{I + \beta \mathbf{W}^T \mathbf{W}} \mathbf{x}_0 - \frac{\beta}{I + \beta \mathbf{W}^T \mathbf{W}} \mathbf{W}^T \mathbf{W} \mathbf{x}_{T-1} \right\|_2^2 \\ &\quad + \left\| \alpha \beta \mathbf{W}^T \mathbf{W} \mathbf{x}_{T-1} - \alpha \beta \mathbf{W}^T T_{\varepsilon(\sigma)}(\mathbf{W} \mathbf{x}_{T-1}) \right\|_2^2 \\ &\leq \left\| \frac{\beta \mathbf{W}^T \mathbf{W}}{I + \beta \mathbf{W}^T \mathbf{W}} \right\|_2^2 \|\mathbf{x}_0 - \mathbf{x}_{T-1}\|_2^2 + \alpha \beta L_{T-1} M \sigma^2 \\ &\leq \alpha \beta \|\mathbf{W}^T \mathbf{W}\|_2^2 \|\mathbf{x}_0 - \mathbf{x}_{T-1}\|_2^2 + \alpha \beta n_{T-1} \sigma^2 \end{aligned} \quad (13)$$

where $n_{T-1} = L_{T-1} M$ is the constant. In the same way, we can get

$$\begin{aligned} &\|\mathbf{x}_0 - \mathbf{x}_{T-1}\|_2^2 \\ &= \|\mathbf{x}_0 - \alpha \mathbf{x}_0 - \alpha \beta \mathbf{W}^T T_{\varepsilon(\sigma)}(\mathbf{W} \mathbf{x}_{T-2})\|_2^2 \\ &= \|\mathbf{x}_0 - \alpha \mathbf{x}_0 - \alpha \beta \mathbf{W}^T \mathbf{W} \mathbf{x}_{T-2} + \alpha \beta \mathbf{W}^T \mathbf{W} \mathbf{x}_{T-2} - \alpha \beta \mathbf{W}^T T_{\varepsilon(\sigma)}(\mathbf{W} \mathbf{x}_{T-2})\|_2^2 \\ &\leq \|\mathbf{x}_0 - \alpha \mathbf{x}_0 - \alpha \beta \mathbf{W}^T \mathbf{W} \mathbf{x}_{T-2}\|_2^2 \\ &\quad + \|\alpha \beta \mathbf{W}^T \mathbf{W} \mathbf{x}_{T-2} - \alpha \beta \mathbf{W}^T T_{\varepsilon(\sigma)}(\mathbf{W} \mathbf{x}_{T-2})\|_2^2 \\ &\leq \left\| \frac{1}{I + \beta \mathbf{W}^T \mathbf{W}} \mathbf{x}_0 - \frac{\beta}{I + \beta \mathbf{W}^T \mathbf{W}} \mathbf{W}^T \mathbf{W} \mathbf{x}_{T-2} \right\|_2^2 \\ &\quad + \left\| \alpha \beta \mathbf{W}^T \mathbf{W} \mathbf{x}_{T-2} - \alpha \beta \mathbf{W}^T T_{\varepsilon(\sigma)}(\mathbf{W} \mathbf{x}_{T-2}) \right\|_2^2 \\ &\leq \left\| \frac{\beta \mathbf{W}^T \mathbf{W}}{I + \beta \mathbf{W}^T \mathbf{W}} \right\|_2^2 \|\mathbf{x}_0 - \mathbf{x}_{T-2}\|_2^2 + \alpha \beta L_{T-2} M \sigma^2 \\ &\leq \alpha \beta \|\mathbf{W}^T \mathbf{W}\|_2^2 \|\mathbf{x}_0 - \mathbf{x}_{T-2}\|_2^2 + \alpha \beta n_{T-2} \sigma^2 \end{aligned} \quad (14)$$

where $n_{T-2} = L_{T-2} M$ is the constant. Following this way, we can obtain

$$\begin{aligned} &\|\mathbf{x}_0 - \mathbf{x}_1\|_2^2 \\ &= \|\mathbf{x}_0 - \alpha \mathbf{x}_0 - \alpha \beta \mathbf{W}^T T_{\varepsilon(\sigma)}(\mathbf{W} \mathbf{x}_0)\|_2^2 \\ &= \|\mathbf{x}_0 - \alpha \mathbf{x}_0 - \alpha \beta \mathbf{W}^T \mathbf{W} \mathbf{x}_0 + \alpha \beta \mathbf{W}^T \mathbf{W} \mathbf{x}_0 - \alpha \beta \mathbf{W}^T T_{\varepsilon(\sigma)}(\mathbf{W} \mathbf{x}_0)\|_2^2 \\ &\leq \|\mathbf{x}_0 - \alpha \mathbf{x}_0 - \alpha \beta \mathbf{W}^T \mathbf{W} \mathbf{x}_0\|_2^2 \\ &\quad + \|\alpha \beta \mathbf{W}^T \mathbf{W} \mathbf{x}_0 - \alpha \beta \mathbf{W}^T T_{\varepsilon(\sigma)}(\mathbf{W} \mathbf{x}_0)\|_2^2 \\ &\leq \left\| \frac{1}{I + \beta \mathbf{W}^T \mathbf{W}} \mathbf{x}_0 - \frac{\beta}{I + \beta \mathbf{W}^T \mathbf{W}} \mathbf{W}^T \mathbf{W} \mathbf{x}_0 \right\|_2^2 \\ &\quad + \left\| \alpha \beta \mathbf{W}^T \mathbf{W} \mathbf{x}_0 - \alpha \beta \mathbf{W}^T T_{\varepsilon(\sigma)}(\mathbf{W} \mathbf{x}_0) \right\|_2^2 \\ &\leq \alpha \beta n_0 \sigma^2 \end{aligned} \quad (15)$$

where $n_0 = L_0 M$ is the constant. The results of each stage are substituted into Eqn. (13), we have

$$\begin{aligned} & \|\mathbf{x}_0 - \mathcal{D}_\theta(\mathbf{x}_0; \sigma)\|_2^2 \\ &= \|\mathbf{x}_0 - \mathbf{x}_T\|_2^2 \\ &\leq \alpha^T \beta^T (\|\mathbf{W}^\top \mathbf{W}\|_2^2)^{T-1} n_0 \sigma^2 \\ &+ \alpha^{T-1} \beta^{T-1} (\|\mathbf{W}^\top \mathbf{W}\|_2^2)^{T-2} n_1 \sigma^2 \\ &+ \dots \\ &+ \alpha^2 \beta^2 (\|\mathbf{W}^\top \mathbf{W}\|_2^2)^1 n_{T-2} \sigma^2 \\ &+ \alpha \beta n_{T-1} \sigma^2. \end{aligned} \quad (16)$$

Since α and β are constants, and $\|\mathbf{W}^\top \mathbf{W}\|_2^2$ is bounded, Eqn. (16) can be further expressed as

$$\begin{aligned} & \|\mathbf{x}_0 - \mathcal{D}_\theta(\mathbf{x}_0; \sigma)\|_2^2 \\ &\leq N_T \sigma^2 + N_{T-1} \sigma^2 + \dots + N_1 \sigma^2 \\ &\leq N \sigma^2 \end{aligned} \quad (17)$$

where N denotes any constant that is not zero, then it means that LipNet satisfies the boundary property. ■

C. The proof of Theorem 2

Based on **Theorem 1**, for all $\mathbf{x}_1, \mathbf{x}_2 \in \mathbb{R}^d$, we can construct the following inequality:

$$\begin{aligned} & \|\mathcal{D}_\theta(\mathbf{x}_1; \sigma) - \mathcal{D}_\theta(\mathbf{x}_2; \sigma)\|_2^2 \\ &= \|\mathbf{x}_1 - \mathbf{x}_1 + \mathcal{D}_\theta(\mathbf{x}_1; \sigma) + \mathbf{x}_2 - \mathbf{x}_2 - \mathcal{D}_\theta(\mathbf{x}_2; \sigma)\|_2^2 \\ &\leq \|\mathbf{x}_1 - \mathbf{x}_2\|_2^2 + \|\mathbf{x}_1 - \mathcal{D}_\theta(\mathbf{x}_1; \sigma)\|_2^2 + \|\mathbf{x}_2 - \mathcal{D}_\theta(\mathbf{x}_2; \sigma)\|_2^2 \\ &\leq \|\mathbf{x}_1 - \mathbf{x}_2\|_2^2 + 2N\sigma^2 \\ &\leq \left(1 + \frac{2N\sigma^2}{\|\mathbf{x}_1 - \mathbf{x}_2\|_2^2}\right) \|\mathbf{x}_1 - \mathbf{x}_2\|_2^2 \\ &\leq v \|\mathbf{x}_1 - \mathbf{x}_2\|_2^2 \end{aligned} \quad (18)$$

where $v = 1 + \frac{2N\sigma^2}{\|\mathbf{x}_1 - \mathbf{x}_2\|_2^2}$ is the Lipschitz constant and $\mathcal{D}_\theta(\cdot; \sigma)$ is v -Lipschitz continuous. ■

D. The proof of Theorem 3

Based on **Theorem 2**, for all $\mathbf{x}_1, \mathbf{x}_2 \in \mathbb{R}^d$, we can construct the following inequality:

$$\begin{aligned} & \|\mathcal{f}_\theta(\mathbf{x}_1; \mathbf{y}) - \mathcal{f}_\theta(\mathbf{x}_2; \mathbf{y})\|_2^2 \\ &= \|\mathcal{D}_\theta(\mathbf{x}_1 + \eta \mathcal{P}^\top(\mathbf{y} - \mathcal{P}\mathbf{x}_1); \sigma) \\ &\quad - \mathcal{D}_\theta(\mathbf{x}_2 + \eta \mathcal{P}^\top(\mathbf{y} - \mathcal{P}\mathbf{x}_2); \sigma)\|_2^2 \\ &\leq v \|\mathbf{x}_1 + \eta \mathcal{P}^\top(\mathbf{y} - \mathcal{P}\mathbf{x}_1) - \mathbf{x}_2 + \eta \mathcal{P}^\top(\mathbf{y} + \mathcal{P}\mathbf{x}_2)\|_2^2 \quad (19) \\ &\leq v (1 - \eta \mathcal{P}^\top \mathcal{P}) \|\mathbf{x}_1 - \mathbf{x}_2\|_2^2 \\ &\leq \underbrace{\max\{|1 - \eta \epsilon|, |1 - \eta \zeta|\}}_{=: \psi} v \|\mathbf{x}_1 - \mathbf{x}_2\|_2^2 \end{aligned}$$

where the network $\mathcal{D}_\theta(\cdot; \sigma)$ is v -Lipschitz, $\epsilon = \delta_{\min}(\mathcal{P}^\top \mathcal{P})$, and $\zeta = \delta_{\max}(\mathcal{P}^\top \mathcal{P})$. Moreover, $\delta_{\min}(\cdot)$ and $\delta_{\max}(\cdot)$ denote the maximum and minimum eigenvalue, respectively. As σ approaches 0, ensuring that v converges to 1 and the coefficient ψ is less than 1, in which case the convergence of the corresponding iterative algorithm for PromptCT is explicitly proved. ■

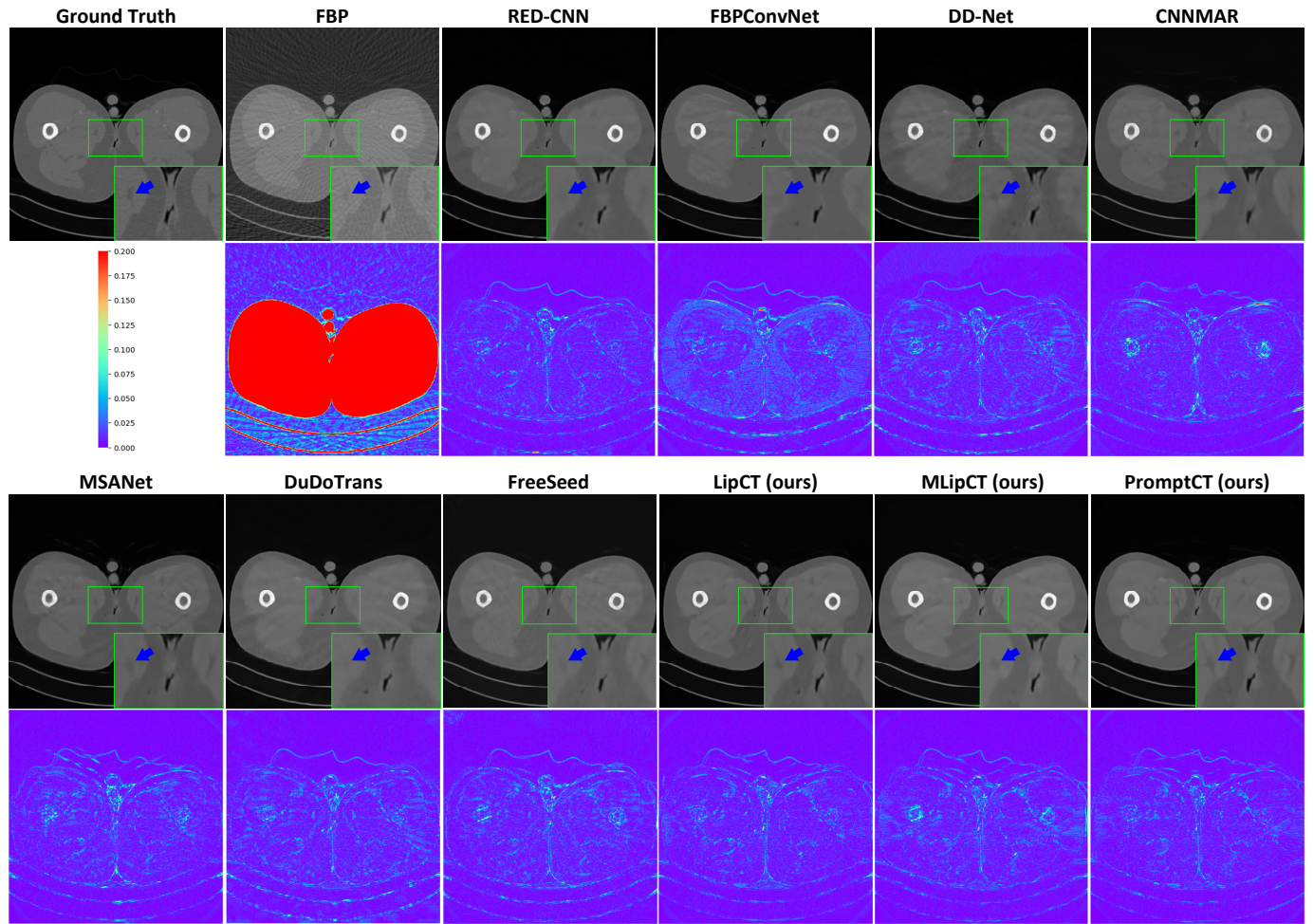


Fig. 2. Reconstruction results with 60 projection views by different SVCT reconstruction algorithms. Regions of interest are zoomed in for better viewing. Below each reconstructed image, we calculate its difference from the original image.

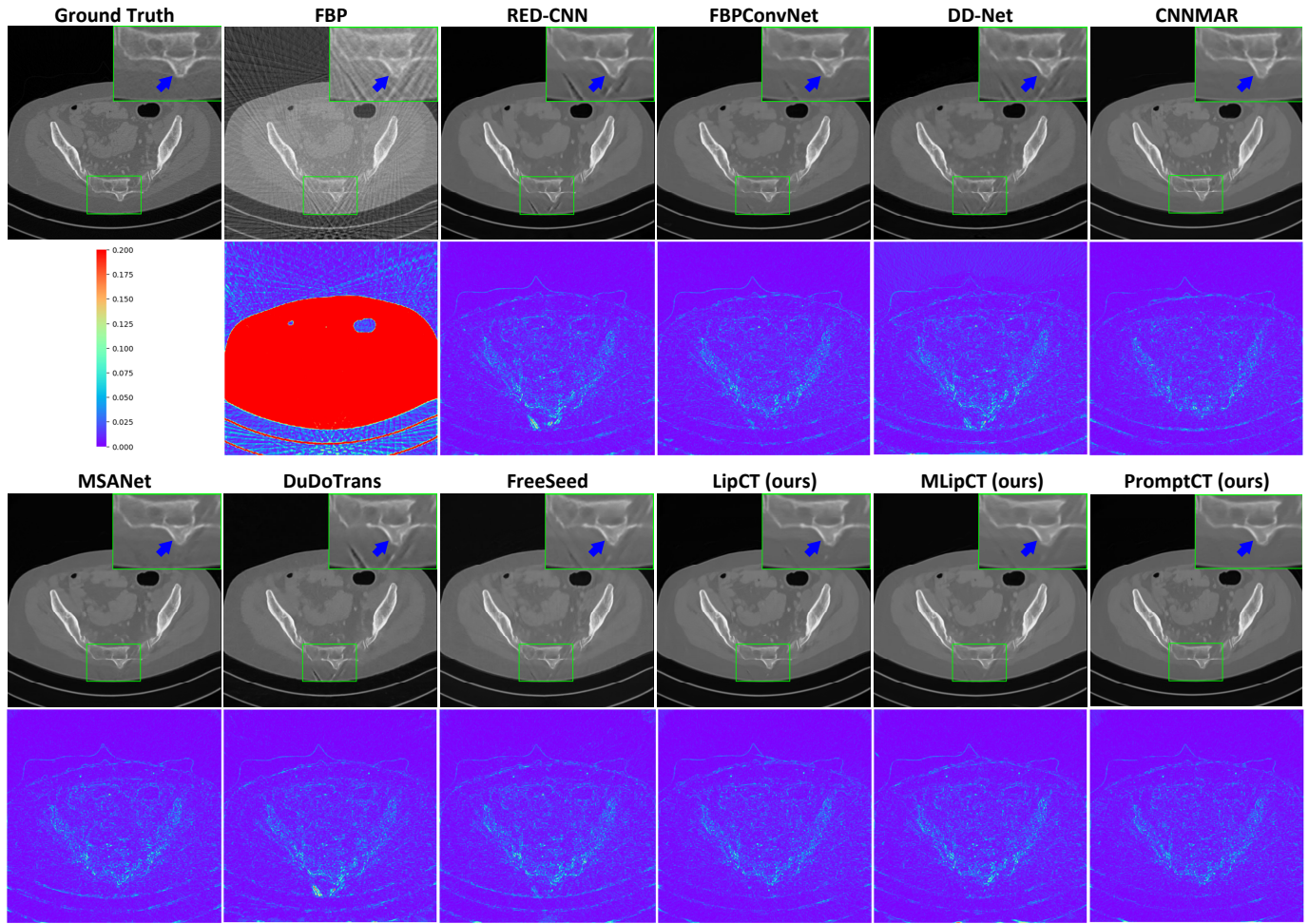


Fig. 3. Reconstruction results with 90 projection views by different SVCT reconstruction algorithms. Regions of interest are zoomed in for better viewing. Below each reconstructed image, we calculate its difference from the original image.

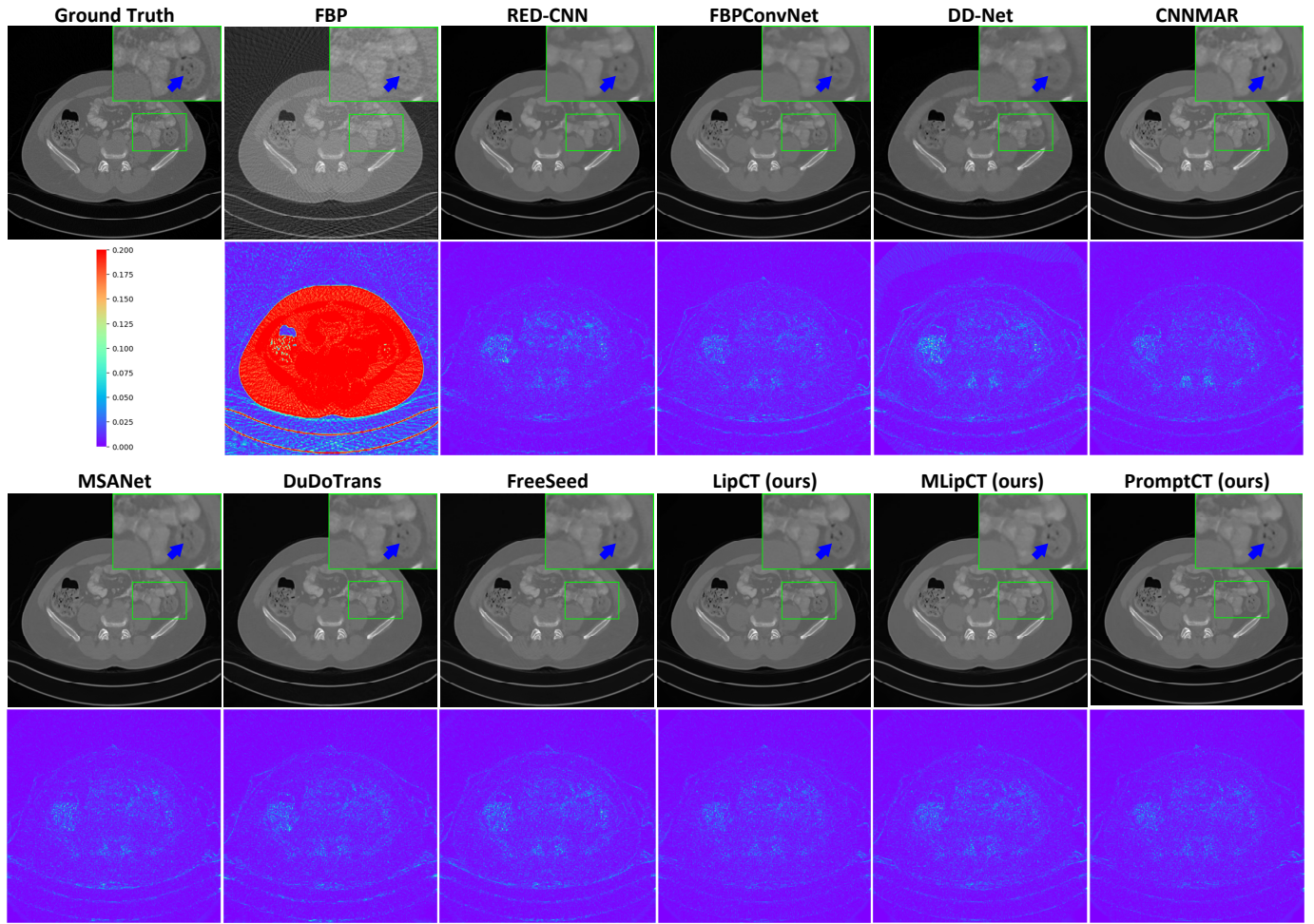


Fig. 4. Reconstruction results with 120 projection views by different SVCT reconstruction algorithms. Regions of interest are zoomed in for better viewing. Below each reconstructed image, we calculate its difference from the original image.

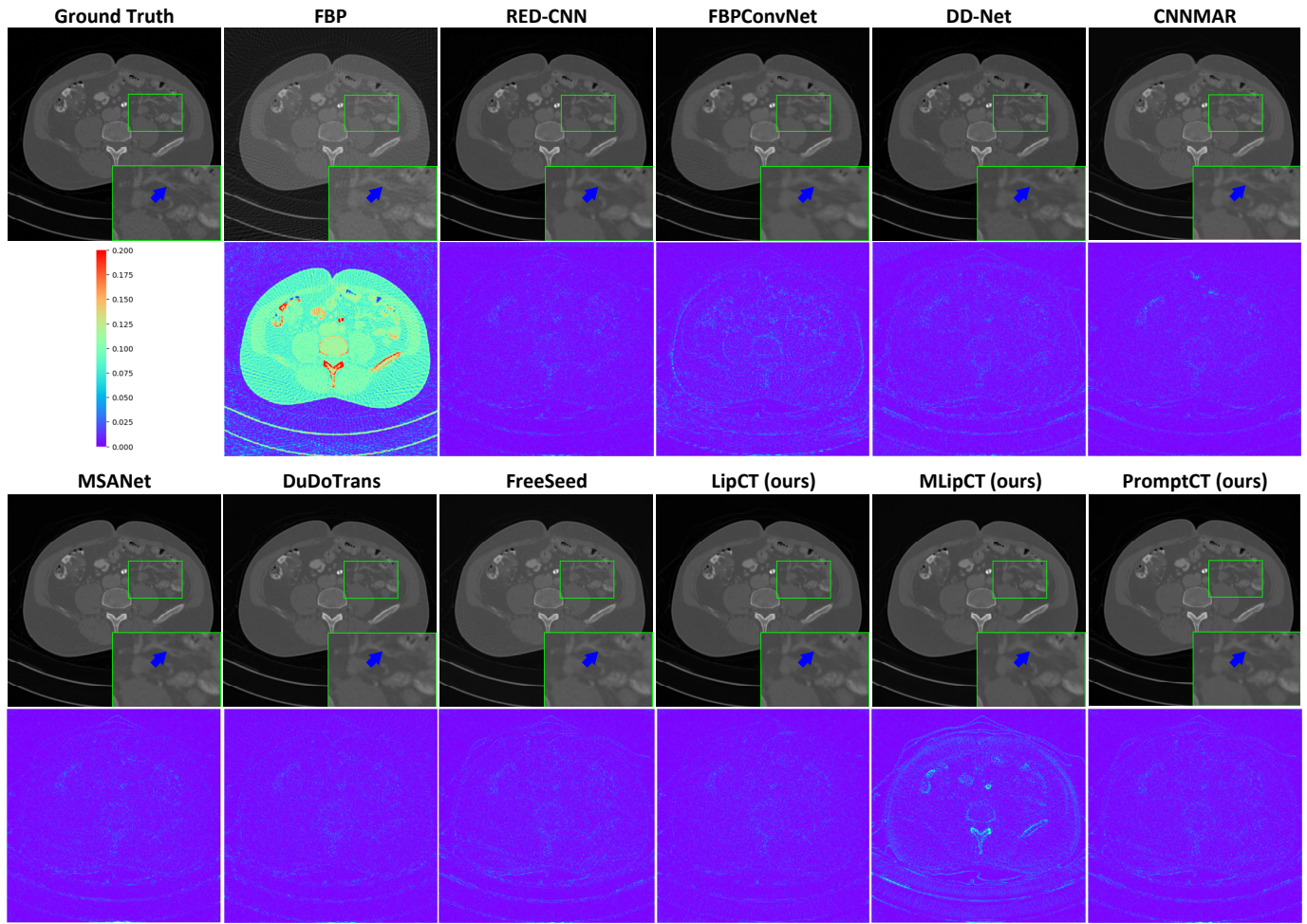


Fig. 5. Reconstruction results with 180 projection views by different SVCT reconstruction algorithms. Regions of interest are zoomed in for better viewing. Below each reconstructed image, we calculate its difference from the original image.